

Characterization of Surface Acetylated Nanocrystalline Cellulose by Single-Step Method

Meiling Yan,^a Shujun Li,^{a,*} Mingxin Zhang,^a Chunjie Li,^a Feng Dong,^{a,b} and Wei Li^c

Surface acetylated nanocrystalline cellulose (NCC) was prepared from cotton fiber by a single-step method under mild conditions using anhydrous phosphoric acid as the solvent. The absorbance peak of O-H was reduced, and the absorbance peaks of C=O and CH₃ appeared in the Fourier transform infrared (FTIR) spectrum of the acetylated NCC with respect to that of the unmodified NCC. The roughly estimated degree of substitution was a little greater than 1.5 by FTIR analyses, implying that most of the free hydroxyl groups on the NCC surface were acetylated at 40 °C for 3 h. The carbons of the acetyl groups were clearly identified in the ¹³C cross polarization-magic angle spinning (CP-MAS) nuclear magnetic resonance (NMR) spectrum. The zeta potential was reduced from -32.12 mV to -20.57 mV after acetylation. Transmission electron microscope (TEM) and field-emission scanning electron microscope (FESEM) images showed that they were thread-like nanocrystals with a diameter less than 5 nm. Crystal structure analysis using X-ray diffraction (XRD) demonstrated that the acetylated NCC had the typical Cellulose II structure. The PLA film reinforced with 3 wt% acetylated NCC content exhibited the highest tensile strength, which was increased by 117% compared to the control. SEM observation demonstrated good interfacial interaction between the acetylated NCC and the matrix.

Keywords: Cotton fiber; Anhydrous phosphoric acid; Acetylation; Nanocrystalline cellulose; Modification; Single-step method

Contact information: a: Key Laboratory of Bio-based Material Science and Technology of Ministry of Education, Northeast Forestry University, Harbin, 150040, P.R. China; b: Light Industry and Textile College, Qiqihar University, Qiqihar, 161006, P.R. China; c: Planning and Design Institute of Forest Products Industry, Beijing, 100010, P.R. China; *Corresponding author: lishujun@nefu.edu.cn

INTRODUCTION

Cellulose is the most abundant biopolymer in the world and widely used at an industrial scale for the manufacture of paper and films or in the following forms: dust, natural, hydrolyzed, or derivatized (Lima *et al.* 2011). Nano-materials have developed very fast. Nano-crystal cellulose (NCC) has also garnered interest from the scientific community because of its renewable nature, abundance, and great properties. Due to a highly order arranged structure and high aspect ratio (length/diameter), rod or thread-shaped nanoscale cellulose has exceptional strength and physicochemical properties and has been used for the preparation of many composites as a reinforced material (Cheng *et al.* 2009; Klemm *et al.* 2011; Dong *et al.* 2012; Huq *et al.* 2012). Sustainability and green issues have stimulated research and development of bio-nanocomposites with this non-petroleum based, biodegradable, high performing and light weight material (Kalia *et al.* 2011). However, it has poor dispersibility / compatibility with non-polar solvents or matrices due to its polar surfaces, which limits its incorporation as a reinforcing material

for nanocomposites only to aqueous or polar systems. To overcome this problem and broaden the application of NCC in other polymer matrices, many studies on modification of NCC have been reported in the past few years. Several new methods, including noncovalent surface chemical modifications, oxidation, acetylation, silylation, sulfonation, carboxylation, cationization, and polymer grafting, have been developed (Hubbe *et al.* 2008; Habibi *et al.* 2010; Peng *et al.* 2011). Among these modification methods, the acetylation reaction is one of the most promising techniques (Jonoobi *et al.* 2012).

There are previous studies on acetylation of NCC but most of them had to utilize multiple processes. Prior to acetylation, the water in NCC suspension must be eliminated because most acetylation reagents could be destroyed by the water. However, the NCCs tend to flocculate by hydrogen bonding after drying because of their high surface area and hydrophilic nature. In order to get an anhydrous reaction system of NCC, a large amount of organic solvent was used to repeatedly replace the water of NCC aqueous suspension (Sassi and Chanzy 1995; Ifuku *et al.* 2007; de Menezes *et al.* 2009), or the NCC aqueous suspension was freeze-dried (Yuan *et al.* 2006; Berlioz *et al.* 2009; Çetin *et al.* 2009; Lin *et al.* 2011). Both of these water-removing processes are very costly and time consuming.

To our best knowledge, the reports by Dorgan's group (Braun and Dorgan 2009; Sobkowicz *et al.* 2009) are the only studies on the acetylation of NCC by a single-step method. By using a mixture of acetic acid, HCl, and organic acids, NCC was isolated and acetylated using the Fischer esterification process. The single-step acetylation method is particularly appealing from both environmental and economic perspectives.

Oksman *et al.* (2006) reported that swelling treatment could make microcrystalline cellulose much more susceptible to separation into nano-fibers. Boerstael *et al.* (2001) found that anhydrous phosphoric acid is an excellent direct solvent for cellulose, which is also cheap and easy to handle. Unlike the homogeneous solution of cellulose with ionic liquid (Matsumura *et al.* 2000; Wu *et al.* 2006; Shakeri and Staiger 2010; Zang *et al.* 2010; Gremos *et al.* 2011), liquid crystalline solutions can be formed when cellulose is dissolved in anhydrous phosphoric acid, and liquid crystalline solutions are known to be good precursors for high modulus/high tenacity yarns (Northolt *et al.* 2001). The cellulose concentration could reach up to 38 wt% after a few minutes. Compared with the concentration of 0.04 g cotton linter/mL acid solution in the report by Dorgan's group, the dissolution in anhydrous phosphoric acid system is very effective. Anhydrous phosphoric acid could also work as a catalyst for esterification (Solomons and Fryhle 2004). Therefore, no other catalyst (*e.g.*, HCl) is needed. However, few reports were found about how NCC was prepared or modified using this system. In our previous report, this system has successfully worked for preparing NCC (Li *et al.* 2013). In this present work, surface acetylated NCC was prepared from cotton fiber by a single-step method using the same system as the solvent, and the acetylated NCC was characterized.

EXPERIMENTAL

Materials

Medical absorbent cotton was of technical grade, made by Yanggu JYG Hygiene & Health Materials Factory, Shandong, China. Other chemicals, such as polyphosphoric acid, phosphoric acid, acetic anhydride, sodium hydroxide, and cellulose acetate were all analytical grade reagents.

Preparation of Acetylated NCC

In this process, polyphosphoric acid and 85% phosphoric acid were mixed in a flask for 1.5 h at 48 °C to prepare an anhydrous phosphoric acid system (P_2O_5 content = 74%) and then cooled down to 1-3 °C (Li *et al.* 2013). Ten grams of medical absorbent cotton was immersed in 90 g of the system, followed by intense kneading with a glass rod and stirring for 2 h to disperse the chemicals and disintegrate the solid cotton. Then, 15 mL of acetic anhydride was added with stirring and kept for 1, 2, or 3 h at 40 °C or for 2 or 3 h at 30 °C, respectively, in order to obtain different acetylated NCC samples. For comparison, another mixture of medical absorbent cotton and anhydrous phosphoric acid system was kept at 40 °C for 3 h without the addition of acetic anhydride to prepare unmodified NCC. Finally, the mixtures were separately poured into icy aqueous NaOH to neutralize the phosphoric acid system, repeatedly centrifuging and dialysis to remove impurities, and the target products were obtained after freeze-drying.

Characterization

Organic functional group analysis

After freeze-drying, the organic functional groups of the unmodified NCC and the acetylated NCC were analyzed with Fourier transform infrared spectroscopy (FTIR). The measurement was carried out using a Nicolet Magna 560 spectrometer with an attenuated total reflectance (ATR) accessory in order to focus on the surface of the NCC samples. The spectra were recorded between 4000 and 650 cm^{-1} with a resolution of 4 cm^{-1} with 32 scans per sample. Degree of substitution (D.S.) of the acetylated cellulose on the crystal surface was roughly compared by FTIR analysis method with some references (Braun and Dorgan 2009; Çetin *et al.* 2009).

Solid state ^{13}C cross polarization-magic angle spinning (CP-MAS) nuclear magnetic resonance (NMR) spectra of the acetylated NCC were recorded at room temperature on a Bruker DRX-400 spectrometer, using a MAS rate of 5 kHz, a contact time of 1000 μs , at a frequency of 75.48 MHz for ^{13}C NMR. The freeze-dried sample was packed in a MAS 4-mm-diameter zirconia rotor. The spectrum was run for 3 h.

State of dispersion of acetylated NCC

The state of dispersion of the unmodified and the acetylated NCC was examined using a Hitachi 7560 Transmission electron microscope (TEM) at 100 KV. A drop of the dilute modified NCC suspension was deposited on carbon-coated grids and allowed to dry at room temperature. The sample was negatively stained with a 2% uranyl acetate aqueous solution for several minutes prior to use.

The state of dispersion of the acetylated NCC was also observed using a FEI Sirion field-emission scanning electron microscope (FESEM) at an accelerating voltage of 20 kV. The freeze-dried sample was sputter-coated with gold before scanning.

Zeta potential and particle size measurements

The hydrodynamic particle sizes and ζ potentials of the unmodified and the acetylated NCC in aqueous solutions were measured at 25 °C using Brookhaven Zeta-Plus Microelectrophoresis Apparatus (Holtsville, NY, USA) and the software of 90 plus/BI-MASS. The scattering angle and operating wavelength were 90° and 658 nm, respectively.

Crystal structure analysis

After removing phosphates and other water soluble substance, the crystal structure of the NCC samples was analyzed using X-ray diffraction (XRD). The measurement was conducted on a D8 ADVANCE XRD in the range of 5° to 80° with a step size of 0.02° at scan speed of 1° s^{-1} .

Preparation of NCC/poly lactide (PLA) Films and Characterization

PLA and NCC/PLA films were prepared by the solvent casting method. PLA (5 g) was dissolved in 50 mL CHCl_3 with vigorous stirring at room temperature. A certain amount of the dissolved solution was poured onto a 15 cm diameter glass Petri dish. After air drying for 1 d, PLA control film was peeled from the Petri dish. For the preparation of the NCC/PLA films, the cellulose powder (unmodified NCC or acetylated NCC) was directly added into chloroform to prepare 2 wt% suspensions. In order to improve the cellulose dispersion in chloroform, the suspensions were exposed to ultrasonication (100 W) for 3 h. Then a predetermined amount of the unmodified or acetylated NCC suspension in chloroform was mixed with the previously prepared PLA solution. NCC/PLA films with 1 wt% to 4 wt% of unmodified NCC or acetylated were prepared by following the same above-described procedure for comparison. The mixed solutions were stirred for 1 d and exposed to ultrasonication (100W) for 30 min before they were cast onto the glass Petri dish (Fortunati *et al.* 2012).

For tensile test, the resultant films with a thickness of ca. $40 \mu\text{m}$ were cut into $10 \text{ mm} \times 100 \text{ mm}$ pieces, and kept for 48 h at 20°C and 65% RH. Along the length, at least ten points were set in the middle to determine the thickness with a micrometer. At least five test samples were tested for each material using an LDX-200 electronic tensile machine for film (Landmark, China) at a strain rate of 10 mm/min , and the averages are presented.

The inner morphological features of the films were investigated by using scanning electron microscopy (SEM, FEI Quanta 200). In order to observe real inner morphological features of the films, the film samples were frozen in liquid nitrogen and then torn into pieces. The new fractures were mounted on a metal stub and sputter-coated with a thin layer of gold for SEM observation.

RESULTS AND DISCUSSION

FTIR Analysis

Figure 1 shows the FTIR spectra of the unmodified and acetylated NCC. A strong band at 3332 cm^{-1} of the unmodified NCC (Fig. 1 Spectrum a) was due to the hydroxyl ($-\text{OH}$) stretching vibration. The absorbance at 2891 cm^{-1} was attributed to symmetric C–H vibrations. A weak band at 1633 cm^{-1} originated from the absorbed moisture of the unmodified NCC. The absorbance at 894 cm^{-1} can be assigned to the C–H deformation mode of the glycosidic linkage between the glucose units. The absorbance between 992 cm^{-1} and 1158 cm^{-1} is attributed to the C–O stretching in major ether bands in NCC (Zaman *et al.* 2012). Compared with the spectrum of the unmodified NCC, three bands in the spectrum of the acetylated NCC (Fig. 1 Spectrum b) were found to be important: 1735 , 1366 , and 1214 cm^{-1} . The three bands are attributed to the C=O stretching, CH_3 in-plane bending, and C–O stretching (ester group), respectively (Sassi and Chanzy 1995; Ifuku *et al.* 2007; Çetin *et al.* 2009; Zang *et al.* 2010; Lima *et al.* 2011). According to the

spectra, the band for hydroxyl groups was largely reduced. Besides, the absorbance peaks for C=O, CH₃, and C–O of ester groups clearly appeared after acetylation, signifying that the NCC was acetylated successfully.

Çetin *et al.* (2009) determined the kinetics of acetylation by calculating the peak height ratio of I_{1740}/I_{1060} in each spectrum. In this work, this method was also used to quantify the extent of acetylation by comparing the intensity of the carbonyl stretching vibration of the grafted acyl group with the 1060 cm⁻¹ vibration associated with C–O stretching of the cellulose backbone, which is used as an internal standard. According to their study, after 6 h acetylation at 94 °C the peak height ratio reached 0.4 and after 24 h they got their highest ration of less than 0.5. In this work, the lowest peak height ratio (0.426) was obtained at 30 °C after only 2 h, and the highest ratio reached 0.501 at 40 °C for 3 h (Table 1). As a comparison, the purchased acetylated cellulose with a *D. S.* of 1.66±0.02 had a peak height ratio of 0.535. Basically, the peak height ratios of I_{1740}/I_{1060} are proportional with the *D.S.* values. The *D.S.* value of the acetylated NCC (40 °C, 3h) was about 1.55. For NCC in Type I crystalline structure, only half of the hydroxyl groups of a surface cellulose molecule in NCC (Cellulose I structure) are accessible, so the maximum *D.S.* is 1.5 (Goussé *et al.* 2002). The maximum *D.S.* for NCC in Type II crystalline structure should be a little larger due to a greater angle ($\gamma=117.3^\circ$). The high *D.S.* value of 1.55 indicates most of the free hydroxyl groups on the surface were acetylated.

Braun and Dorgan (2009) conducted a quantitative evaluation of FTIR through normalization of the absorbance peak area of the carbonyl carbon of the ester at 1736 cm⁻¹ with the area underneath the absorbance peak centered at 1162 cm⁻¹, which corresponds to the C–O–C stretch of the ring structure of the cellulose repeat unit. The normalization proceeds according to the following equation:

$$\frac{\alpha_{1736}}{\alpha_{1162}} = \frac{e(1736)c_E}{e(1162)c_R} = B \frac{c_E}{c_R} = B(N_{E,RU}) \quad (1)$$

In Eq. 1, α_{1736} and α_{1162} are the areas underneath the peaks centered at a wave number 1736 and 1162 cm⁻¹, respectively, with a new baseline established between 2000 and 777 cm⁻¹, c_E and c_R represent the concentrations of the ester groups and cellulose ring structures, and $N_{E,RU}$ represents the number of esters per cellulose repeat unit, *i.e.*, the *D. S.* value. The molar absorptivities $e(1736)$ and $e(1162)$ are wavelength-specific material constants (for the carbonyl carbon of the ester group at 1736 cm⁻¹ and the C–O–C cellulose ring stretch at 1162 cm⁻¹), so the ratio value B is also a constant. Using this method, the lowest $N_{E,RU}$ (1.53) was obtained at 40 °C for 1 h, and the highest $N_{E,RU}$ (1.68) at 40 °C for 3 h. All the values of $N_{E,RU}$ were a little greater than 1.5, also signifying that most of the free hydroxyl groups on the surface were acetylated.

Table 1. Calculated *D.S.* and $N_{E,RU}$ under Different Acetylation Conditions

No.	Temperature (°C)	Time (h)	I_{1740}/I_{1060}	Calculated <i>D.S.</i> by I_{1740}/I_{1060}	$N_{E,RU}$
1	40	1	0.482	1.49	1.53
2	40	2	0.486	1.51	1.56
3	40	3	0.501	1.55	1.68
4	30	3	0.470	1.46	1.60
5	30	2	0.426	1.32	1.58
0	--	--	0.535	1.66*	1.66*

*It was defined, not calculated.

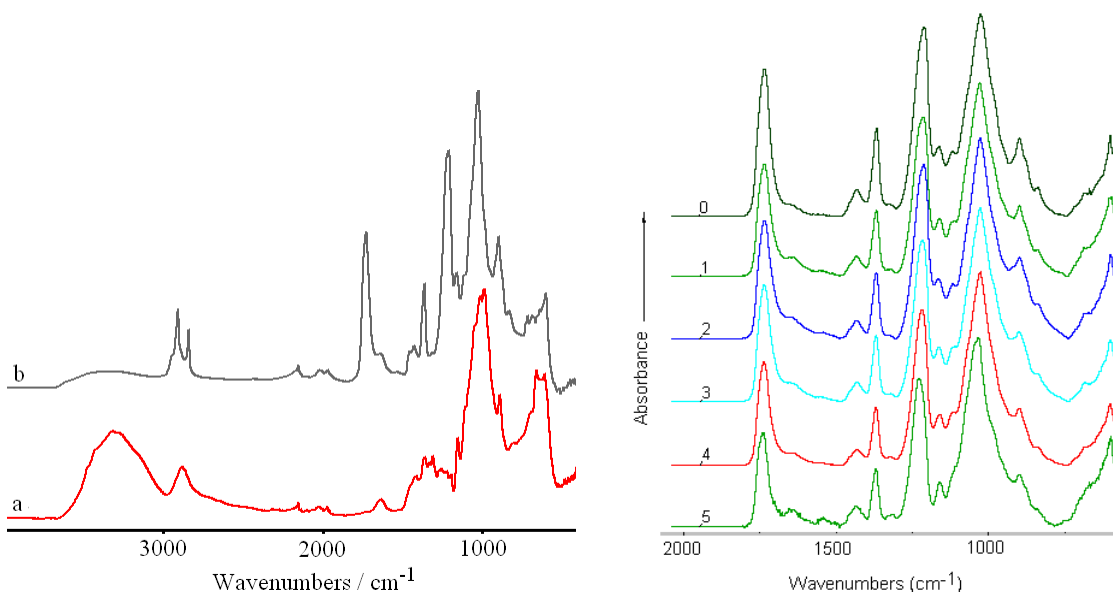


Fig. 1. FTIR spectra of unmodified NCC (a), acetylated NCC (b); Details of the acetylated NCC under different conditions: (0-purchased comparison, 1-reaction at 40 °C for 1 h, 2-at 40 °C for 2 h, 3-at 40 °C for 3 h, 4-at 30 °C for 3 h, 5-at 30 °C for 2 h)

¹³C CP-MAS NMR Spectroscopy

The unmodified NCC and the acetylated NCC were further characterized by ¹³C CP-MAS NMR spectroscopy (Fig. 2). The chemical shifts at 50 to 100 ppm were identified as the spinning bands arising from the glucose unit carbons. The carbons of the acetyl groups were clearly identified at 163 and 14 ppm (carbons α and β , respectively, according to the nomenclature in Fig. 2), further confirming the success of the acetylation.

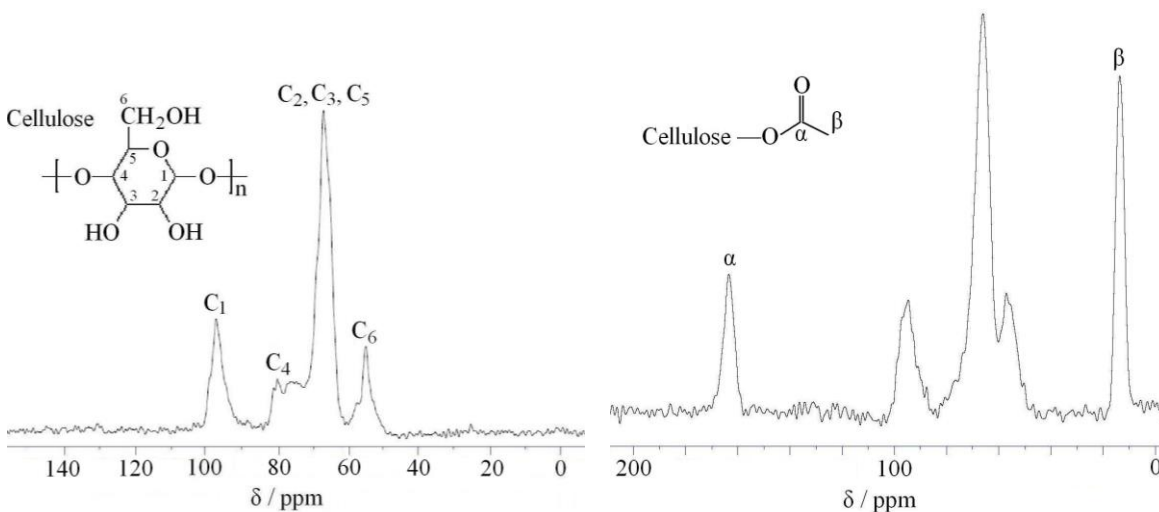


Fig. 2. ¹³C CP-MAS NMR spectra of the unmodified ¹³C NCC (left) and the acetylated NCC (right)

Çetin *et al.* (2009) reported that the intensities of the α and β carbon resonances increased gradually with reaction time when they acetylated freeze-dried cellulose nanowhiskers with vinyl acetate at 94 °C. Intensities of the α and β carbon resonances of the acetylated NCC (40 °C, 3 h) in this work are significantly higher than those in their report, even their longest reaction time was 24 h. This indicates that the acetylation method presented in this work is very efficient.

TEM Analysis

Figure 3 shows the TEM images of the unmodified NCC and the acetylated NCC. Obviously, the cotton fiber had been turned into thread-like nano-crystals by the anhydrous phosphoric acid system. Most were well dispersed, and undispersed big bundles could hardly be found. It has been well known that the hydrolysis of cellulose from various sources with strong sulfuric acid or hydrochloric acid under controlled condition gives a suspension of rod-like or thread-like nano-cellulose crystals, whose length falls within the size range of 200 to 500 nm and width of 5 to 10 nm (Beck-Candanedo *et al.* 2005). However, both the unmodified and the acetylated cellulose crystals were very thin and their diameters were in range of 3 to 5 nm. This also indicates that the anhydrous phosphoric acid system has great ability to disperse cotton fiber.

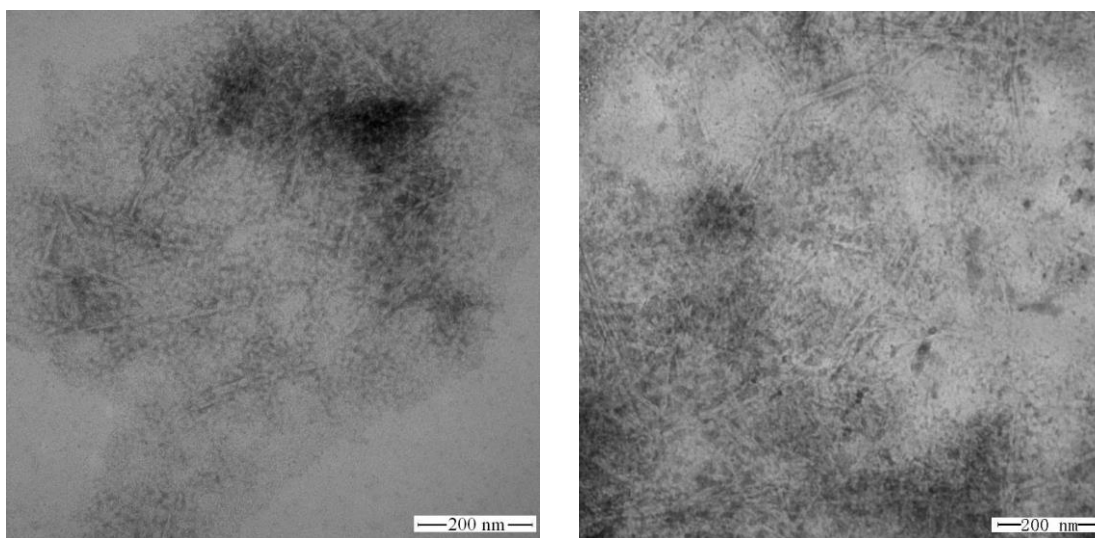


Fig. 3. TEM images of the unmodified NCC (left) and the acetylated NCC (right)

FESEM Analysis

Figure 4 is the FESEM image of the acetylated NCC.

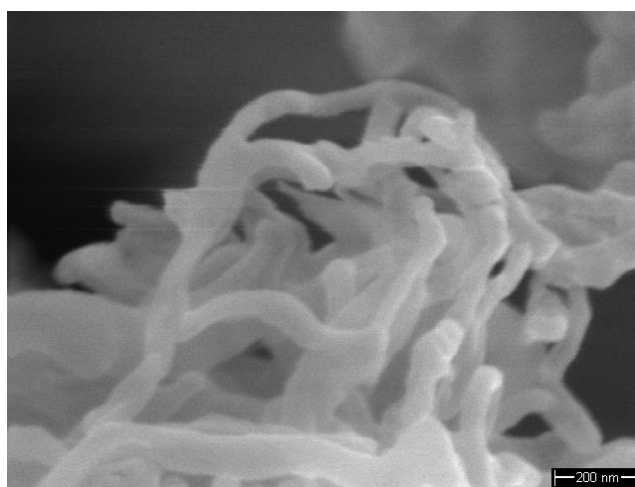


Fig. 4. FESEM image of the acetylated NCC

Due to the process of freeze-drying and then sputter-coating with gold, the diameter of acetylated NCC was much bigger than those in the TEM image above. Apart from this, the thread-like nanomorphology is consistent with that in the TEM image.

Zeta Potential and Particle Size Change

Cellulose shows negative potential on its surface. After modification, some free hydroxyl groups were acetylated, resulting in a reduction of ζ potential (Hubbe and Rojas 2008). In this work, the ζ potential was significantly decreased from -32.12 ± 1.67 mV to -20.57 ± 1.88 mV by acetylation, which indicates that the NCC was surface acetylated.

Due to small size and very high specific surface area, NCC has a tendency to form aggregates in various systems (Zaman *et al.* 2012). Sulfuric acid hydrolyzed cellulose nanocrystals have negatively charged sulfate ester groups on its surface that provide electrostatic stabilization. NCC obtained from hydrochloric acid hydrolysis or others lacks surface charges and often form flocculates or bundles in various systems. In this work, the particle size of the unmodified NCC was 253.4 ± 21.6 nm, and the particle size of the acetylated NCC was 266.1 ± 8.7 nm. This implies that the size of NCC was not changed by the acetylation reaction in the single-step method.

XRD Analysis

In the XRD patterns (Fig. 5), there were high peaks appearing at about 12.4° , 20.5° , and 22.2° , in which 12.4° and 20.5° were due to the 101 side, and 22.2° was due to the 002 side of cellulose. All the characteristic peaks demonstrate that both the unmodified NCC and the acetylated NCC had the typical Cellulose II structure, which is in good agreement with previous reports (Kim *et al.* 2006; Li and Sheng 2009; Shakeri and Staiger 2010). In general, natural cellulose has a Type I structure. Many treatments of cellulose into ionic liquids convert microcrystalline cellulose into amorphous cellulose (Kim *et al.* 2006; Wu *et al.* 2006; Zang *et al.* 2010; Gremos *et al.* 2011; Lima *et al.* 2011). In this process, the treatment with anhydrous phosphorus acid turned the crystal structure into Cellulose II, which demonstrates that the anhydrous phosphorus acid reached the inner part of the original Cellulose I crystals. After the phosphorus acid was removed, the cellulose chains were tightly assembled again and formed Cellulose II crystals. Basically, the acetylation did not change the crystalline structure.

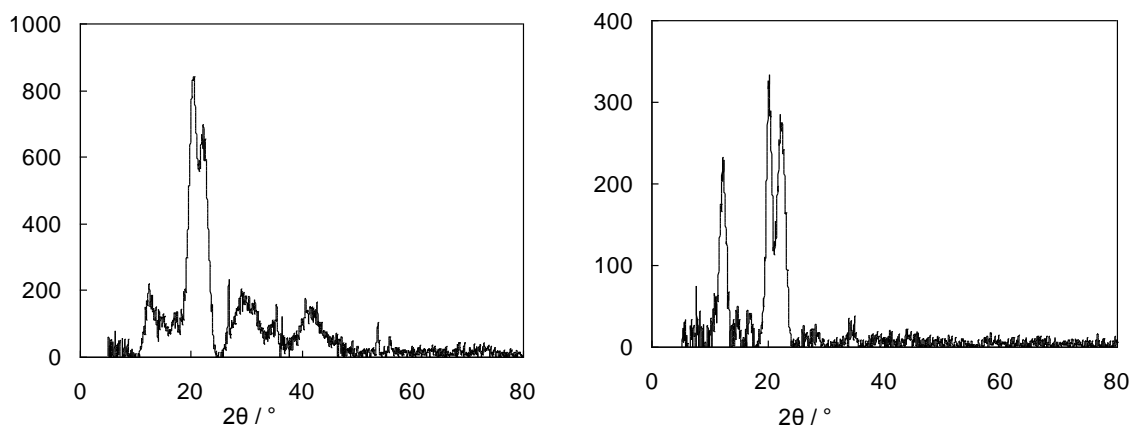


Fig. 5. XRD patterns of the unmodified NCC (left) and the acetylated NCC (right)

In the previous work by de Menezes *et al.* (2009), the NCC remained semicrystalline after chemical modification by grafting organic acid chlorides and displayed a Cellulose I XRD pattern. However, a new ill-defined peak appeared around 21° . The cited authors judged that the peak was attributable to the presence of grafted aliphatic chains. Considering the XRD pattern of the acetylated NCC, their peak at 21° is more like a sign that their modified NCC has been partially converted into Cellulose II.

Reinforcement of NCC Samples to PLA Film

Although the reinforcement performance of Cellulose II has been demonstrated by Northolt *et al.* (2001) and Phuong and Lazzeri (2012), few reports on the reinforced materials by Cellulose II nano-crystals could be found, not to mention those by acetylated Cellulose II nano-crystals. Therefore, the acetylated NCC reinforced PLA film was prepared and characterized with the unmodified NCC reinforced PLA for comparison. Their reinforcement effect is illustrated in Fig. 6.

As expected, the acetylated NCC worked better than the unmodified NCC for reinforcing PLA film. The PLA film reinforced with 3% acetylated NCC content exhibited the highest tensile strength (23.59 MPa), which was increased by 117% compared to the control. The film with 3% unmodified NCC content was also reinforced about 97% compared to the control, but the tensile strength was only close to that of the film with 2% acetylated NCC.

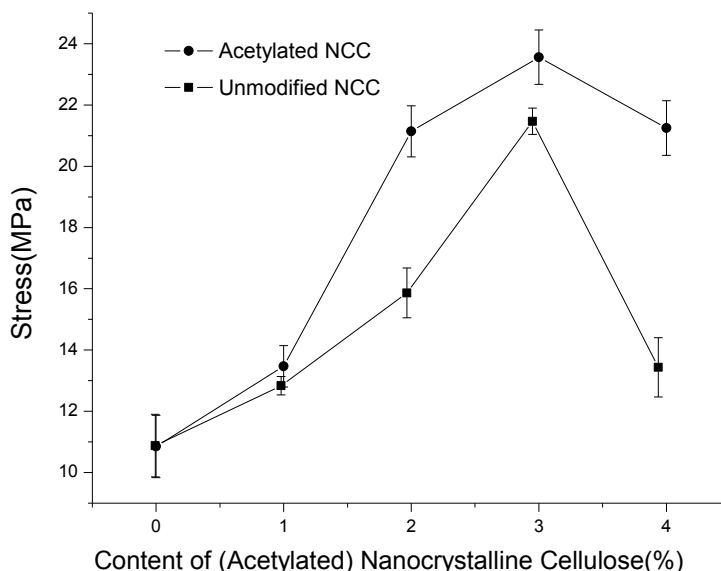


Fig. 6. Effect of NCC content (wt%) on tensile stress (MPa) of PLA film

Figure 7 shows the SEM images of the reinforced films on cross section. Obviously, the biggest difference between the two images is many holes in the unmodified NCC/PLA section, but no holes were present in the acetylated NCC reinforced PLA film, indicating great interface compatibility between the acetylated NCC and the PLA matrix.

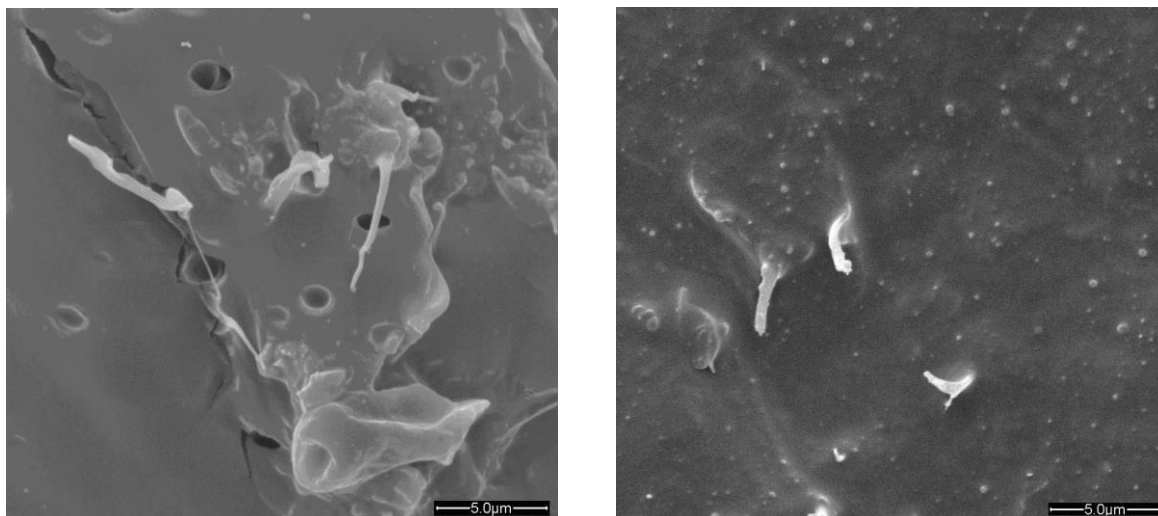


Fig. 7. SEM images of the unmodified NCC/PLA film (left) and the acetylated NCC/PLA film (right)

CONCLUSIONS

1. A single-step method for preparation and acetylation of NCC is presented. Cotton fiber was disintegrated in anhydrous phosphoric acid and successfully acetylated by acetic anhydride. Under mild conditions, surface acetylated NCC was obtained.
2. FTIR and ^{13}C CP-MAS NMR analyses confirm the NCC was acetylated successfully. The roughly estimated degree of substitution by FTIR analysis was a little greater than 1.5, signifying most of the free hydroxyl groups on crystal surface were acetylated. TEM and FESEM images prove that the acetylated NCCs were thread-like nano-crystals. The zeta potential reduced from -32.12 mV of the unmodified NCC to -20.57 mV. XRD patterns demonstrate that the acetylated NCC had the typical Cellulose II structure due to anhydrous phosphoric acid system.
3. The acetylated nano-crystals in Cellulose II structure increased PLA by 117% at a content of only 3 wt%. SEM images elucidated that there is good interfacial interaction between the acetylated NCC and the matrix.

ACKNOWLEDGEMENT

The authors are grateful for the support of the Chinese Fundamental Research Funds for the Central Universities, Grant. No. DL11EB01 and valuable suggestions from Dr. Todd F. Shupe from Louisiana State University, USA.

REFERENCES CITED

- Beck-Candanedo, S., Roman, M., and Gray, D. G. (2005). "Effect of reaction conditions on the properties and behavior of wood cellulose nanocrystal suspensions," *Biomacromolecules* 6(2), 1048-1054.
- Berlitz, S., Molina-Boisseau, S., Nishiyama, Y., and Heux, L. (2009). "Gas-phase

- surface esterification of cellulose microfibrils and whiskers,” *Biomacromolecules* 10(8), 2144-2151.
- Braun, B., and Dorgan, J. R. (2009). “Single-step method for the isolation and surface functionalization of cellulosic nanowhiskers,” *Biomacromolecules* 10(2), 334-341.
- Boerstoel, H., Maatman, H., Westerink, J. B., and Koenders, B.M. (2001). “Liquid crystalline solutions of cellulose in phosphoric acid,” *Polymer* 42(17), 7371-7379.
- Çetin, N. S., Tingaut, P., Özmen, N., Henry, N., Harper, D., Dadmun, M., and Sèbe, G. (2009). “Acetylation of cellulose nanowhiskers with vinyl acetate under moderate conditions,” *Macromol. Biosci.* 9(10), 997-1003.
- Cheng, Q., Wang, S., and Rials, T. G. (2009). “Poly(vinyl alcohol) nanocomposites reinforced with cellulose fibrils isolated by high intensity ultrasonication,” *Compos. Part A: Appl. S.* 40(2), 218-224.
- de Menezes, A. Jr., Siqueira, G., Curvelo, A. A. S., and Dufresne, A. (2009). “Extrusion and characterisation of functionalised cellulose whiskers reinforced polyethylene nanocomposites,” *Polymer* 50(19), 4552-4563.
- Dong, H., Strawhecker, K. E., Snyder, J. F., Orlicki, J. A., Reiner, R. S., and Rudie, A. W. (2012). “Cellulose nanocrystals as a reinforcing material for electrospun poly(methyl methacrylate) fibers: Formation, properties and nanomechanical characterization,” *Carbohydr. Polym.* 87(4), 2488-2495.
- Fortunati, E., Peltzer, M., Armentano, I., Torre, L., Jiménez, A., and Kenny, J. M. (2012). “Effects of modified cellulose nanocrystals on the barrier and migration properties of PLA nano-biocomposites,” *Carbohydr. Polym.* 90 (2), 948-956.
- Gremos, S., Zarafeta, D., Kekos, D., and Kolisis, F. (2011). “Direct enzymatic acylation of cellulose pretreated in BMIMCl ionic liquid,” *Bioresource Technol.* 102(2), 1378-1382.
- Goussé, C., Chanzy, H., Excoffier, G., Soubeyrand, L., and Fleury, E. (2002). “Stable suspensions of partially silylated cellulose whiskers dispersed in organic solvents,” *Polymer* 43(9), 2645-2651.
- Habibi, Y., Lucia, L. A., and Rojas, O. J. (2010). “Cellulose nanocrystals: Chemistry, self-assembly, and applications,” *Chem. Rev.* 110(6), 3479-3500.
- Hubbe, M. A., Rojas, O. J., Lucia, L. A., and Sain, M. (2008). “Cellulosic nanocomposites: A review,” *BioResources* 3(3), 929-980.
- Hubbe, M. A., and Rojas, O. J. (2008). “Colloidal stability and aggregation of lignocellulosic materials in aqueous suspension,” *BioResources* 3(4), 1419-1491.
- Huq, T., Salmieri, S., Khan, A., Khan, R. A., Tien, C. L., Riedl, B., Fraschini, C., Bouchard, J., Uribe-Calderon, J., Kamal, M. R., and Lacroix, M. (2012). “Nanocrystalline cellulose (NCC) reinforced alginate based biodegradable nanocomposite film,” *Carbohydr. Polym.* 90(4), 1757-1763.
- Ifuku, S., Nogi, M., Abe, K., Handa, K., Nakatsubo, F., and Yano, H. (2007). “Surface modification of bacterial cellulose nanofibers for property enhancement of optically transparent composites: Dependence on acetyl-group DS,” *Biomacromolecules* 8(6), 1973-1978.
- Jonoobi, M., Mathew, A. P., Abdi, M. M., Makinejad, M. D., and Oksman, K. (2012). “A comparison of modified and unmodified cellulose nanofiber reinforced polylactic acid (PLA) prepared by twin screw extrusion,” *J. Polym. Environ.* 20(4), 991-997.
- Kalia, S., Kaith, B. S. and Kaur, I. (2011). *Cellulose fibers: Bio- and nano-polymer composites*, Springer-Verlag Berlin Heidelberg.
- Kim, C.-W., Kim, D.-S., Kang, S.-Y., Marquez, M., and Joo, Y. L. (2006). “Structural

- studies of electrospun cellulose nanofibers,” *Polymer* 47(14), 5097-5107.
- Klemm, D., Kramer, F., Moritz, S., Lindström, T., Ankerfors, M., Gray, D., and Dorris, A. (2011). “Nanocelluloses: A new family of nature-based materials,” *Angew. Chem. Int. Ed.* 50(24), 5438-5466.
- Li, L., and Sheng, G. (2009). “Analysis on crystalline structure of cellulose fiber from cotton-straw bast by X-ray diffraction method,” *J. Cell. Sci. Technol.* 17(4), 37-40,52.
- Lima, G. M., Sierakowski, M.-R., Faria-Tischer P. C. S., and Tischer, C. A. (2011). “Characterisation of bacterial cellulose partly acetylated by dimethylacetamide / lithium chloride,” *Mater. Sci. Eng. C* 31(2), 190-197.
- Lin, N., Huang, J., Chang, P. R., Feng, J., and Yu, J. (2011). “Surface acetylation of cellulose nanocrystal and its reinforcing function in poly(lactic acid),” *Carbohydr. Polym.* 83(4),1834-1842.
- Matsumura, H., Sugiyama, J., and Glasser, W. G. (2000). “Cellulosic nanocomposites. I. Thermally deformable cellulose hexanoates from heterogeneous reaction,” *J. Appl. Polymer Sci.* 78(13), 2242-2253.
- Northolt, M. G., Boerstoel, H., Maatman, H., Huisman, R., Veurink, J., and Elzerman H. (2001). “The structure and properties of cellulose fibres spun from an anisotropic phosphoric acid solution,” *Polymer* 42(19), 8249-8264.
- Oksman, K., Mathew, A.P., Bondeson D., and Kvien, I. (2006). “Manufacturing process of cellulose whiskers / polylactic acid nanocomposites,” *Compos. Sci. Tech.* 66(15), 2776-2784.
- Peng, B. L., Dhar, N., Liu, H. L., and Tam, K. C. (2011). “Chemistry and applications of nanocrystalline cellulose and its derivatives: A nanotechnology perspective,” *Can. J. Chem. Eng.* 89(5), 1191-1206.
- Phuong, V. T., and Lazzeri, A. (2012). “‘Green’ biocomposites based on cellulose diacetate and regenerated cellulose microfibrils: Effect of plasticizer content on morphology and mechanical properties,” *Compos. Part A-Appl. S.* 43(12), 2256-2268.
- Sassi, J. and Chanzy, H. (1995). “Ultrastructural aspects of the acetylation of cellulose,” *Cellulose* 2(2), 111-127.
- Shakeri, A., and Staiger, M. P. (2010). “Phase transformations in regenerated microcrystalline cellulose following dissolution by an ionic liquid,” *BioResources* 5(2), 979-989.
- Sobkowicz, M. J., Braun, B., and Dorgan, J. R. (2009). “Decorating in green: Surface esterification of carbon and cellulosic nanoparticles,” *Green Chem.* 11(5), 680-682.
- Solomons, T. W. G., and Fryhle, C. B. (2004). *Organic Chemistry*, Chichester: Wiley, New York.
- Wu, J., Zhang, H., Zhang, J., and He, J. (2006). “Homogeneous acetylation and region-selectivity of cellulose in a new ionic liquid,” *Chem. J. Chinese U.* 27(3), 592-594.
- Yuan, H., Nishiyama, Y., Wada, M., and Kuga, S. (2006). “Surface acylation of cellulose whiskers by drying aqueous emulsion,” *Biomacromolecules* 7(3), 696-700.
- Zaman, M., Xiao, H., Chibante, F., and Ni, Y. (2012). “Synthesis and characterization of cationically modified nanocrystalline cellulose,” *Carbohydr. Polym.* 89(1), 163-170.
- Zang, H., Zhang, Y., Zang, Y., Cheng, B., Song, J., Ji, K., and Chang, J. (2010). “Study on the homogeneous acetylation of cellulose in a mixed ionic liquid of [AMMor]Cl / [AMIm]Cl,” *Acta Chim. Sinica* 68(3), 283-287.

Article submitted: January 20, 2013; Peer review completed: April 25, 2013; Revised version received and accepted: October 17, 2013; Published: October 22, 2013.